

Dynamical properties of a Haldane-gap antiferromagnet

This article has been downloaded from IOPscience. Please scroll down to see the full text article.

1993 J. Phys.: Condens. Matter 5 1399

(<http://iopscience.iop.org/0953-8984/5/9/024>)

View [the table of contents for this issue](#), or go to the [journal homepage](#) for more

Download details:

IP Address: 171.66.16.96

The article was downloaded on 11/05/2010 at 01:11

Please note that [terms and conditions apply](#).

Dynamical properties of a Haldane-gap antiferromagnet

O Golinelli, Th Jolicœur† and R Lacaze‡

Service de Physique Théorique‡, CE Saclay, F-91191 Gif-sur-Yvette Cédex, France

Received 1 December 1992

Abstract. We study the dynamic spin correlation function of a spin-1 antiferromagnetic chain with easy-plane single-ion anisotropy. We use exact diagonalization by the Lanczós method for chains of length up to $N = 16$ spins. We show that a single-mode approximation is an excellent description of the dynamical properties. A variational calculation allows us to clarify the nature of the excitations. The existence of a two-particle continuum near-zero wavevector is clearly seen, both in finite-size effects and in the dynamical structure factor. The recent neutron scattering experiments on the quasi-one-dimensional antiferromagnet NENP are fully explained by our results.

1. Introduction

It was first argued by Haldane [1, 2] that generic spin- S one-dimensional Heisenberg antiferromagnets have an excitation gap for integer S . This picture is quite different from the usual, higher-dimensional, picture of antiferromagnets with massless Goldstone magnons. On the theoretical side, there is now convincing evidence from numerical studies [3–10] of the $S = 1$ Heisenberg chain that it has a non-zero gap in the thermodynamic limit. Exact diagonalizations by the Lanczós method have been able to reach 18 spins, and Monte Carlo simulations extend the range to 32 spins. All these data are suggestive of a Haldane gap. This leads to a ground-state spin correlation length which is finite and about six lattice spacings. Such a picture is in striking contrast to the $S = 1/2$ solvable chain, which is gapless and whose ground state has algebraically decaying correlations. A spin-1 Heisenberg model with biquadratic exchange has also been discovered with an exactly solvable ground state and a non-zero gap [11], thus reinforcing the belief in the Haldane conjecture.

On the experimental side, there are several candidates to exhibit this quantum gap. The first experimental evidence came from neutron scattering on the compound CsNiCl_3 [12–15]. In this compound there are chains of spin-1 Ni^{2+} ions with superexchange through Cl^- anions. There are, however, moderately small interchain couplings that complicate the picture: this is revealed in recent experiments on the related compound RbNiCl_3 [16]. The best candidate so far seems to be $\text{Ni}(\text{C}_2\text{H}_8\text{N}_2)_2\text{NO}_2\text{ClO}_4$ (NENP) [17–20], as shown by inelastic neutron scattering (INS) and magnetization measurements. The ratio of the interchain to intrachain magnetic coupling is estimated to be $J'/J \approx 4 \times 10^{-4}$. No transition to Néel order is found down to 1.2 K, which is consistent with the hypothesis of a *finite* zero-temperature

† CNRS Research Fellow.

‡ Laboratoire de la Direction des Sciences de la Matière du Commissariat à l'Énergie Atomique.

correlation length. Nickel ions have spin one, and are described by the following anisotropic Heisenberg Hamiltonian [21]:

$$H = J \sum_i \mathbf{S}_i \cdot \mathbf{S}_{i+1} + D \sum_i (S_i^z)^2. \quad (1.1)$$

A best fit of INS gap values leads to $J/k_B = 43.5$ K and easy-plane $D/J = 0.18$ [10]. There is also evidence for a smaller in-plane anisotropy that can be described by adding to H a term $E \sum_i [(S_i^x)^2 - (S_i^y)^2]$. This perturbation is small and will be mostly ignored in the remainder of this paper. Its qualitative role will be discussed in section 5.

The first INS measurements [17–19] have concentrated on the neighbourhood of $Q = \pi$ (where Q is the wavevector along the chain) and showed the existence of two gaps: one for the in-plane (IP) magnetic fluctuations and a higher one for out-of-plane (OP) fluctuations. This splitting is due to the presence of a sizable easy-plane single-ion anisotropy D . The dispersion of the magnetic excitations was then studied in the range $Q/\pi = 0.9$ – 1.0 . Recent experiments have extended our knowledge throughout the whole Brillouin zone [22]. Detailed theoretical work is required to test the hypothesis that the simple model Hamiltonian (1.1) is able to reproduce the dynamical properties of NENP. Two approaches have been followed up to now: small-cluster numerical studies [3–10, 23] and the use of effective-field theories [24, 25]. The previous numerical studies were limited to spectral calculations or have ignored the presence of in-plane anisotropy.

In this paper we present the results of a study of the dynamical structure factor $S(Q, \omega)$ of chains of length up to 16 spins by means of an exact diagonalization method. We also apply a variational technique proposed in [26] to the anisotropic chain. This physically motivated method reproduces extremely well the numerical results. The results presented are valid in the absence of an external magnetic field and in the zero-temperature limit, i.e. for temperatures well below the gap. In section 2 we present some general properties of the spin-1 chain with easy-plane single-ion anisotropy. In section 3 we explain the methods used to obtain dynamical quantities. Section 4 contains our results. They are extremely well reproduced in terms of a physically appealing single-mode approximation. The results of our variational calculation are presented there, and we use them to understand the nature of the elementary excitations near $Q = 0$ and $Q = \pi$. We show in section 5 that they are in very good agreement with existing neutron data, and we suggest an additional test of the theory. Section 6 contains our conclusions.

2. General properties

We briefly review some known results about the isotropic Heisenberg spin-1 antiferromagnetic (AF) chain:

$$H_0 = J \sum_{i=1}^N \mathbf{S}_i \cdot \mathbf{S}_{i+1}. \quad (2.1)$$

The vectors \mathbf{S}_i are quantum spin operators satisfying the SU(2) rotation algebra with length $S_i^2 = 2$. They are located along a one-dimensional lattice of N sites

with periodic boundary conditions. The exchange integral J is positive in the AF case. For any finite lattice the ground state is a singlet and the higher-lying levels have energy increasing with increasing spin, as is known rigorously [27]. Above the singlet ground state one finds a triplet state, presumably for all values of N . In an AF quantum magnet, in the case of broken symmetry, one expects that in the thermodynamic limit the triplet becomes degenerate with the ground state as do other states with spin $S = 2, 3, \dots$, in order to form the degenerate ground state of the infinite-volume limit. This can occur only for dimensions greater than or equal to 2. Haldane has argued that the spin-1 chain is quantum disordered and that the singlet-triplet gap remains non-zero in the thermodynamic limit. This should be true for any integer value of the spin. This argument is based on a mapping of the infinite-spin semiclassical limit of the quantum chain onto an $O(3)$ non-linear σ model [1]. In the spin-1 case of interest, numerical studies clearly point towards a gap close to $\approx 0.41J$ [3–10, 23]. The physics of the $O(3)$ non-linear σ model is that of a triplet of massive bosons with non-trivial scattering properties. This suggests a very simple effective-field theory: a free theory of three massive bosons [25]. Another route, starting from an integrable model, leads to an effective-field theory of three massive fermions [24].

In such approaches one has to adjust the gap values, which are no longer deducible from the microscopic model, but one can obtain simple and definite predictions on dynamical quantities. However, both are approximate theories and their respective domains of validity are difficult to assess. On the other hand, finite-chain calculations offer unbiased theoretical predictions provided one is able to carefully control finite-size effects. Concerning the gap values this can be achieved by the use of the so-called Shanks transformation, suited to the removal of exponential transients in sequences of finite-chain data [28]. It has been found that the convergence towards infinite volume is very good [6, 10, 23], which is as expected since we are dealing with a massive theory. We are in a situation where the spin correlation length, ≈ 6 lattice spacings, is already smaller than the longest chains we use.

As shown with the Perron-Frobenius theorem [29], the lowest-lying triplet has wavevector $Q = \pi$, while the singlet ground state has $Q = 0$. Most theoretical and experimental studies have concentrated on this $Q = \pi$ part of the spectrum. In the non-linear σ model, there are no bound states and, if we believe that it is the effective theory of the spin-1 chain, this implies that the $Q = 0$ gap is due to two massive $Q = \pi$ particles and thus twice the $Q = \pi$ gap [2]. This has been checked by a quantum Monte Carlo simulation in the isotropic case [8] and Lanczós studies [23] have shown that this property persists in the presence of anisotropy (as long as it is not too large). As a consequence, the states near $Q = 0$ should be members of a two-particle continuum, contrary to the states near $Q = \pi$ that should appear as long-lived well defined excitations. INS measurements for $Q = 0$ [30] reveal a vanishing structure factor in this regime. The curve of the lowest excited triplet at wavevector Q is thus bell shaped, but asymmetrical with respect to $Q = \pi/2$.

Let us now discuss the influence of easy-plane single-ion anisotropy, i.e. adding to H_0 a term of the following form:

$$H = H_0 + D \sum_i (S_i^z)^2. \quad (2.2)$$

The full rotational symmetry of Hamiltonian (2.1) is broken to rotational symmetry around the z axis. Only the z component $S^z = \sum_i S_i^z$ of the total spin is conserved.

There is also a discrete symmetry $S^z \rightarrow -S^z$ that is preserved in the Hamiltonian (2.2). As a consequence of the anisotropy, the first excited triplet state is split into a higher-energy singlet, $S^z = 0$, and a lower-lying doublet, $S^z = \pm 1$. These three states retain their wavevectors unchanged ($Q = \pi$) with respect to the $D = 0$ case (by continuity) since the Hamiltonian (2.2) still possesses translational symmetry. The Haldane gap is split into two components: one gap $G^{(-)}$ between the ground state (with $S^z = 0$) and the doublet $S^z = \pm 1$ and one gap $G^{(+)}$ inside the $S^z = 0$ subspace between the first two levels. The gap $G^{(-)}$ decreases while $G^{(+)}$ increases with increasing D , as shown quantitatively in [10].

We expect this simple picture to be true for all wavevectors $0 \leq Q \leq \pi$ since the triplet states with arbitrary Q will also be split by the anisotropy. There are thus two distinct magnetic modes throughout the Brillouin zone: one IP (in-plane) mode (doubly degenerate) and one OP (out-of-plane) mode. The IP mode is seen in the $S^z = \pm 1$ sector while the OP mode appears in the $S^z = 0$ sector. The dispersion of the IP mode has been obtained for various anisotropies, including that of NENP in [23]. INS experiments [17–19, 22] have resolved these two modes in the neighbourhood of $Q = \pi$: the OP mode is found at 2.5 meV, and the IP mode is even further resolved into two components at 1.05 meV and 1.25 meV. This splitting is due to a small in-plane anisotropy of the type $E \sum_i [(S_i^x)^2 - (S_i^y)^2]$ that lifts the degeneracy of the doublet states $S^z = \pm 1$. These values of the gaps (ignoring the in-plane anisotropy) lead to $J = 44$ K and $D/J = 0.18$ [10]. Detailed interpretation of INS requires a calculation of the structure factor $S(Q, \omega)$.

3. Evaluating dynamical quantities

We describe in this section the methods used to compute the dynamical structure factor

$$S^{\alpha\alpha}(Q, \omega) = \int dt e^{i\omega t} \langle 0 | S_{-Q}^{\alpha}(t) S_Q^{\alpha}(0) | 0 \rangle \quad \alpha = x, y, z. \quad (3.1)$$

Here we denote the ground state by $|0\rangle$ and the components of the Fourier transform of the spin vectors are $S_Q^{\alpha}(t)$ in the Heisenberg representation. We first write the structure factor as

$$S^{\alpha\alpha}(Q, \omega) = \sum_n \delta(\omega - (\epsilon_n - \epsilon_0)) |\langle n | S_Q^{\alpha} | 0 \rangle|^2 \quad (3.2)$$

where the sum over $|n\rangle$ means over all excited eigenstates of the system and ϵ_n denotes the energy of $|n\rangle$. In a finite-system calculation, one obtains a finite set of delta functions with weights given by the matrix elements appearing in (3.2). The Lanczós method, which is commonly used to obtain the ground-state wavefunction and the first few excited levels, is suited to the study of the dynamical properties [31].

We proceed as follows.

(i) One needs to know first the vector $|0\rangle$. We use the Lanczós algorithm applied to the Hamiltonian H . In fact, any kind of algorithm can be used at this level.

(ii) One constructs the state

$$|\Phi_0\rangle = S_Q^{\alpha} |0\rangle. \quad (3.3)$$

This state $|\Phi_0\rangle$ is then used to build a new Lanczós sequence of states $|\Phi_n\rangle$ by the standard procedure of applying the Hamiltonian to $|\Phi_k\rangle$ and orthonormalization with respect to the last two vectors $|\Phi_k\rangle$ and $|\Phi_{k-1}\rangle$. The Hamiltonian H is then tridiagonal in the basis $\{|\Phi_n\rangle\}$. The non-zero elements of H in this basis are directly provided by the orthonormalization procedure. We exhaust the corresponding subspace and store the tridiagonal form of the Hamiltonian.

(iii) One diagonalizes the tridiagonal Hamiltonian by a standard routine. This leads to a set of eigenenergies, ϵ_n , as well as the eigenvectors whose first coordinate in the Lanczós basis are precisely the overlap matrix elements $\langle n|\Phi_0\rangle$ that appear in the definition of the structure factor (3.2). We thus obtain the weight of each delta function peak. This has to be done separately for each Q as well as for $\alpha = x, z$.

In the isotropic $D = 0$ case the ground state is a singlet: $S_{Q=0}^\alpha|0\rangle = 0$ and thus $S^{\alpha\alpha}(Q = 0, \omega) = 0$. The vanishing with Q will occur quadratically. In the presence of easy-plane anisotropy the ground state is invariant only under z rotations: $S_{Q=0}^z|0\rangle = 0$ and thus $S^{zz}(Q = 0, \omega) = 0$, while $S^{xx}(= S^{yy})$ will be non-zero at $Q = 0$ and $O(D^2)$. With in-plane anisotropy $E \sum_i [(S_i^x)^2 - (S_i^y)^2]$, even $S^{zz}(Q = 0)$ will be non-zero and $O(E^2)$.

4. Results for $S(Q, \omega)$

We have computed the structure factors $S^{xx}(Q, \omega)$ and $S^{zz}(Q, \omega)$ for chains of lengths $N = 4, 6, 8, 10, 12, 14, 16$. Some $Q = 0$ and $Q = \pi$ parts of the spectrum have also been computed for $N = 18$. We have concentrated on the case $D/J = 0.18$, which is quantitatively relevant to the study of NENP. Our results extend smoothly for not too large anisotropy, $D < J$. For $D = 0$ we reproduce previous findings [8] concerning the lowest excited levels. Previous Monte Carlo measurements of the dynamical structure factor [9] for $D = 0$ are also compatible with our data.

According to the definition (3.2), we will first discuss the peak positions and then the corresponding weights. What we observe is that for all fixed wavevector Q , as a function of ω the lowest-lying peak concentrates almost all of the spectral weight. This remark will be made quantitatively precise at the end of this section. This lowest-lying peak occurs when the frequency ω matches the energy of the first excited level with the right quantum numbers.

In the correlation S^{xx} we find the excitation spectrum from $S^z = 0$ to $S^z = \pm 1$ that we obtained previously [23]. This is plotted in figure 1 as a function of the momenta by crosses of various sizes. For $Q = 0$ and $Q = \pi$ there are enough data to allow an extrapolation to the thermodynamic limit by use of the Shanks transformation. We have also computed these gaps ($Q = 0$ and $Q = \pi$) for a $N = 18$ chain. The extrapolation leads to $0.301J$ at $Q = \pi$ and $0.986J$ at $Q = 0$. In the interval $[0, \pi]$ there is only the middle of the Brillouin zone $Q = \pi/2$, where we obtain several data points from $N = 4, 8, 12, 16$. A Shanks extrapolation leads then to $2.75J$ for $Q = \pi/2$.

In the correlation S^{zz} we find the excitation spectrum inside the $S^z = 0$ subspace. The lowest-lying excitation is plotted in figure 1 with empty octagons. At $Q = \pi$ the finite-lattice data extrapolate to $0.655J$. The convergence in this case, $Q = \pi$, is very good, as expected from a massive theory yielding well separated eigenvalues in the finite systems [23]. On the contrary, at $Q = 0$ the convergence is extremely bad and one can only suggest a value of $0.60 \pm 0.05J$ for this gap. This is clearly due

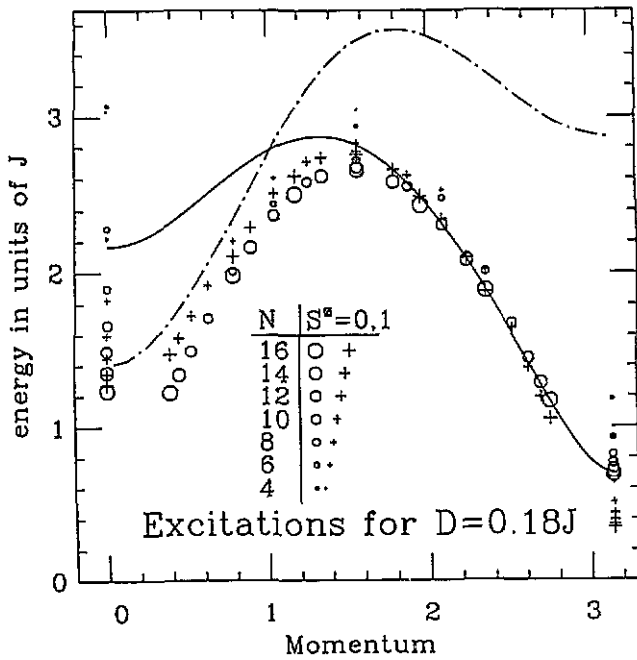


Figure 1. Dispersion of magnetic excitations $S^z = 0$ and $S^z = \pm 1$ from the Lanczos calculations for chain lengths $N = 4, 6, 8, 10, 12, 14, 16$. The energy is in units of J and the momenta range from 0 to π . The full curve is the result of a variational calculation. The chain curve is the corresponding edge of two-particle excitations.

to the presence of a continuum of states starting immediately above this gap. Such a phenomenon is expected if one describes the spectrum near $Q = 0$ as due to two particles with momenta near $Q = \pi$ [8].

We note that the excitations in this sector (zz) are above the in-plane excitations in the neighbourhood of $Q = \pi$, but they cross for $Q/\pi \approx 0.75$ and on the top of the dispersion curve it is the in-plane mode that has highest energy: $2.75J$ against $2.65J$ (extrapolated value) for the out-of-plane mode. This behaviour persists in the region $0 \leq Q \leq \pi/2$ of the Brillouin zone.

To gain understanding of the nature of the excitations we have performed a variational calculation along the lines proposed by Gómez-Santos [26]. One discards the states with parallel spins, either if they are nearest neighbours or separated by any number of zeros. The typical states in this subspace are of the form

$$|\dots \uparrow \uparrow \uparrow 0 \downarrow 00 \uparrow \downarrow \dots\rangle. \quad (4.1)$$

There is strict Néel ordering of the $S^z = \pm 1$ sites, but there can be any number of intermediate zeros. In this subspace the true degrees of freedom are then the 'spin-zero defects' i.e. sites with $S_i^z = 0$. These domain walls are then represented as fermions (which is a natural way of enforcing no double occupancy). The fermionic Hamiltonian can then be treated by approximate methods. It has been shown that a simple Hartree-Fock decoupling leads to a good approximation of the spectrum for $D = 0$. The best results are obtained by using the variational improvement introduced by Gómez-Santos, where one allows a small admixture of states with parallel spins. The Haldane gap, as computed by this method, is found to be $0.45J$ for $D = 0$. It is straightforward to include anisotropy of the form $D \sum_i (S_i^z)^2$. We have obtained a spectrum of massive fermions $E(Q)$, plotted as a continuous curve in figure 1. This curve should be the excitation spectrum in the $S^z = 0$ subspace due to the restriction to the subspace (4.1). The gap at $Q = \pi$ is found to be $\approx 0.70J$ when $D/J = 0.18$.

The single-fermion curve $E(Q)$ reproduces extremely well the OP dispersion in the region $\pi/2 < Q < \pi$. The IP dispersion will be discussed later.

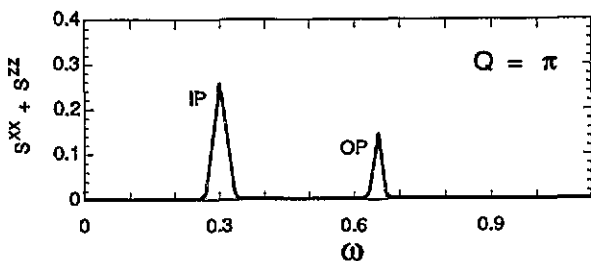


Figure 2. The structure factor $S^{(xx)}(Q = \pi, \omega) + S^{(zz)}(Q = \pi, \omega)$ as a function of the frequency ω (in units of J) for chain length $N = 16$. Each of the two functions $S^{(\alpha\alpha)}$ has a single-peak structure: a single-mode approximation works very well. The IP mode is doubly degenerate and appears only in $S^{(xx)}$ while the OP appears in $S^{(zz)}$.

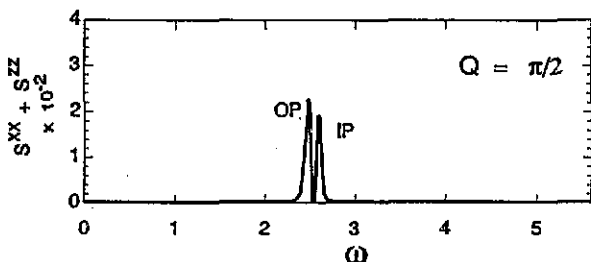


Figure 3. The structure factor $S^{(xx)}(Q = \pi/2, \omega) + S^{(zz)}(Q = \pi/2, \omega)$ as a function of the frequency ω (in units of J). Note that the IP and OP modes are interchanged with respect to the $Q = \pi$ case (figure 2).

We now turn to a discussion of the spectral weight associated with the peak positions. For all chain lengths studied, for all wavevectors in the interval $[\approx 0.3-1.0]\pi$, we find that both S^{xx} and S^{zz} are dominated by a single peak as a function of the frequency. This peak concentrates at least 98% of the spectral weight. Multimagnon contributions are thus extremely small in the whole range $[\approx 0.3-1.0]\pi$. As typical examples we plot in figure 2 $S^{xx}(Q = \pi, \omega) + S^{zz}(Q = \pi, \omega)$ from the $N = 16$ chain. The peaks have been broadened for clarity. In figure 3 we plot the $Q = \pi/2$ case showing the interchange of the two modes. A single-mode approximation will be an extremely good description of the physics in this part of the Brillouin zone. The simple picture described above breaks down for small values of Q . In the $N = 16$ chain, for $Q = 3\pi/8$ there is still the one-peak structure, while for $Q = \pi/4$ there are several peaks as a function of ω : see figure 4. In the $N = 14$ chain we find that the continuum appears already for $Q = 2\pi/7$ but is not there for $3\pi/7$. It is difficult to give a precise value of the wavevector at which this phenomenon appears since the discretization of the momenta imposed by the chain length is coarse. As discussed below, this can be interpreted as evidence for a two-particle continuum. Our present data suggest that the continuum sets in at $\approx 0.3\pi$ for both IP and OP sectors. We see no reason why the continuum boundary should be the same for both modes, although we are unable to see any quantitative difference in our present data between IP and OP modes in this respect.

Let us now discuss the nature of the two-particle excitations. If a single-particle excitation has a dispersion $E(Q)$, the lower edge of the continuum of two-particle excitations is given by $E^{(2)}(Q) = \min_K (E(K) + E(Q - K))$ in the non-interacting case. Such a free picture seems to apply to the spin-1 chain [1, 2, 24]. In the

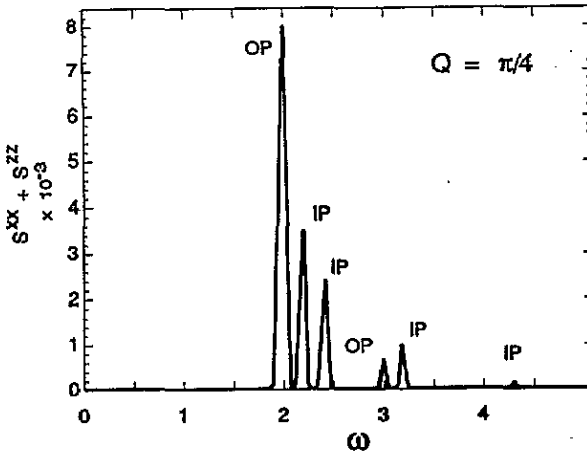


Figure 4. The structure factor $S^{(xx)}(Q = 0.25\pi, \omega) + S^{(zz)}(Q = 0.25\pi, \omega)$ for $N = 16$. Here a single-mode approximation no longer holds and the two-particle continuum is seen: spectral weight is transferred to multimagnon excitations.

anisotropic system it is possible to construct several continua since there are two distinct modes (IP and OP).

In the $S^z = \pm 1$ subspace two-particle states are obtained from one $S^z = \pm 1$ excitation and one $S^z = 0$ excitation. The gap of this continuum at $Q = 0$ will be the sum of the IP and the OP gap at $Q = \pi$, i.e. $\approx 0.301J + 0.655J$ in agreement with our extrapolation of $0.986J$. The continuum is also seen in the poor convergence of finite-size data. Its progressive build-up is seen in figure 4.

In the $S^z = 0$ subspace there are two ways of building two-particle states: either with two $S^z = 0$ states or with one excitation $S^z = +1$ and one excitation $S^z = -1$. In the first case we can obtain an approximation for the continuum boundary by using the fermionic method cited above: the curve $E^{(2)}(Q)$ for two fermionic excitations belonging to the $S^z = 0$ sector is plotted as a chain curve in figure 1. The two-fermion continuum is clearly above the OP (and IP) mode for $0 < Q < \pi/2$. However, the second possibility is that the continuum ($S^z = +1$) + ($S^z = -1$) has a $Q = 0$ gap that is twice the gap at $Q = \pi$ for the IP mode, i.e. $\approx 0.6J$. This agrees with our estimate $\approx 0.6J$ for the gap in the OP sector at $Q = 0$. This continuum is thus the lowest-lying one. This reasoning shows also that the OP ($S^z = 0$) mode should be below the IP mode for $Q \approx 0$, since the IP gap is then given by $\approx 0.301J + 0.655J$. In fact, as stressed above, we have good evidence that the crossing of the two modes occurs quite near $Q/\pi \approx 0.75$.

The agreement between the *ab initio* data and the variational calculation confirms the relevance of domain walls in the whole Haldane phase, as is also pointed out in [32]. The disordered-flat phases obtained in the solid-on-solid picture of the spin-1 chain [33] also correspond to the subspace of spin-zero defects, which is so successful in the description of the elementary excitations.

Finally we quote results for the static structure factors $S^{(\alpha\alpha)}(Q)$ obtained by integration over frequency. In figure 5 these quantities are plotted on a logarithmic scale as a function of momentum. Due to our limited chain length, we cannot make any firm statement about the prediction [1] of square-root Lorentzian behaviour near $Q = \pi$. Our data are compatible with previous studies [34, 35], pointing to a correlation length ≈ 6 lattice spacings in the $D = 0$ case: the correlation length does not change much when $D/J = 0.18$. The behaviour of $S^{(zz)}(Q) \approx Q^2$ sets in only for very small wavevectors: for the largest part of the Brillouin zone, except in the

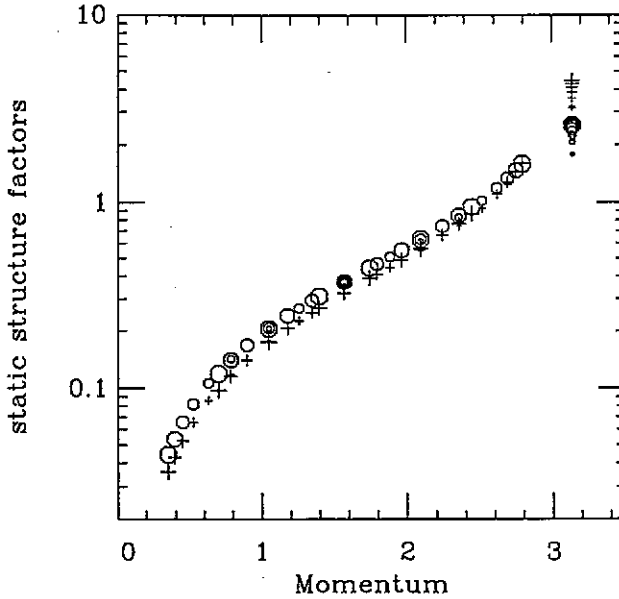


Figure 5. The static structure factors $S^{(xx)}$ and $S^{(zz)}$ for all chain lengths as a function of momentum. The symbol sizes are the same as in figures 1 and 6. Crosses stand for $S^{(xx)}$ and octagons for $S^{(zz)}$.

neighbourhood of $Q = \pi$, it is rather close to $Q^{3/2}$.

5. Comparison with neutron scattering experiments

The two magnetic modes in the neighbourhood of $Q = \pi$ have been observed by INS in [17–20]. The values of the gaps lead to $J \approx 3.8 \text{ meV}$ and $D/J = 0.18$. These values are very close to those extracted from magnetization measurements [36]. The dispersion has been studied throughout the whole Brillouin zone [22]. A good fit is obtained through the following formula:

$$\omega_{\pm}(Q) = [\Delta_{\pm}^2 + v^2 \sin^2(Q) + A^2 \cos^2(\frac{1}{2}Q)]^{1/2}. \quad (5.1)$$

The parameters are $\Delta_+ = 2.5 \text{ meV}$, $\Delta_- = 1.2 \text{ meV}$, $v = 9.6 \text{ meV}$ and $A = 6.1 \text{ meV}$. Scaling by $J = 4 \text{ meV}$ we plot $\omega_{\pm}(Q)$ as full curves in figure 6. For clarity we have also plotted our Lanczós points. The edges of the two-particle continuum extracted from the fits (5.1) are also plotted in figure 6. The lower broken curve corresponds to the $(S^z = +1) + (S^z = -1)$ continuum, while the upper broken curve corresponds to $(S^z = +1) + (S^z = 0)$.

There is good agreement with theoretical results in the neighbourhood of $Q = \pi$, where the IP and OP modes are separated by the experimental resolution [17–20, 22]. In the region $\pi/2 < Q < \pi$ the fits (5.1) are also in agreement with the theoretical results. The two modes are no longer separated since they are very close to each other. At the top of the dispersion curve $Q = \pi/2$ we estimate the gaps, from the values quoted in section 4, to be $2.75J$ for the IP mode and $2.65J$ for the OP.

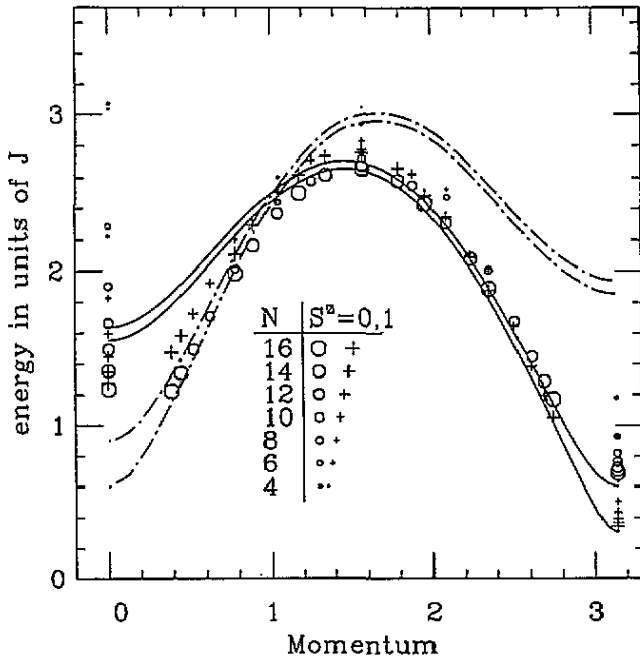


Figure 6. Lanczós results compared to experimental fits. The two full curves are taken from (5.1). They reproduce the findings of [22]. The two chain curves are the two-magnon continuum boundaries obtained also from (5.1). The size of the symbols is chosen as in figure 1.

This means that the IP mode is at ≈ 11 meV and the OP mode at ≈ 10.5 meV using the value of J quoted above. The crossing (or near crossing) of the two modes for $Q \approx 0.75\pi$ precludes their separation in this region of Q . In the regime $Q < \pi/2$ the separation of the modes increases, but the intensity of the scattering decreases strongly, as is seen from figure 5. The continuum will appear for $Q < 0.3\pi$ and is not seen in present experiments [22]. We see it for $Q = 0.25\pi$ and below, but there the structure factor will be very small. For the whole interval $0.3\pi - 1.0\pi$ our data are well reproduced by long-lived excitations as is seen experimentally [22]. The asymmetry with respect to $\pi/2$ of the spectrum (figures 1 and 6) demonstrates the absence of broken translational symmetry. The trend of the magnetic intensity against Q in figure 5 is that found by INS [22]. Absence of data for Q very close to π forbids us to check the square-root Lorentzian behaviour expected for each of the static functions $S^{(xx)}$ and $S^{(zz)}$.

With respect to what has already been done, it would be very interesting to separate the two modes near $\pi/2$ where intensity is not dramatically weak. The observation of the two-particle continuum, on the other hand, should be quite difficult since it appears only for $Q < 0.25\pi$, where magnetic scattering is very weak. The observation of very long-lived modes [22] is thus in very good agreement with the physics of an anisotropic spin-1 chain.

Finally we comment on the uncertainties in the numerical data. For the gap values there is very good convergence for $Q = \pi$ and there one can use all the chain lengths at our disposal. For other values of Q it is only at the top of the spectrum that an

extrapolation can be performed. Concerning the values of Q at which something interesting happens (e.g. crossing of the two modes or entering the continuum) without being able to make refined extrapolations we can only observe that they do not depend much on the chain length. The corresponding numbers should be regarded as tentative (i.e. 0.75π for the crossing and 0.3π for the continuum).

High-resolution INS experiments [30] have revealed that the IP mode is split by in-plane anisotropy $E \sum_i [(S_i^x)^2 - (S_i^y)^2]$. Our results, neglecting this further splitting, will thus apply to the description of actual experiments as long as the resolution is not very high. This effect is not expected to change greatly the numerical figures.

6. Conclusion

We have studied the dynamical properties of a spin-1 chain with single-ion easy-plane anisotropy, thought to be relevant to the magnetic behaviour of the compound NENP. The dynamical structure factor $S^{(\alpha\alpha)}(Q, \omega)$ has been computed by a Lanczós method on chains of length up to 16 spins, while some parts of the spectrum have been obtained on an 18-spins chain. We have performed a variational calculation to obtain the spectrum of elementary excitations in the $S^z = 0$ sector. Both *ab initio* and approximate methods agree very well, elucidating the role of spin-zero defects in the Haldane phase.

We find that the magnetic excitations are described by two distinct long-lived modes throughout most of the Brillouin zone $0.3\text{--}1.0\pi$, where the lowest excited state in each sector ($S^z = 0$ and $S^z = \pm 1$) carries almost all of the spectral weight: a single-mode approximation is thus adequate. We find that these modes merge into a two-particle continuum for $Q < 0.3\pi$, as seen in the frequency dependence of the structure factor. We have shown that these results reproduce the INS experiments on NENP. The dispersion of the magnetic modes as well as their intensity is close to that found theoretically.

Our results show that in principle it should be possible to observe the crossing of the two IP and OP magnetic modes. At the top of the dispersion curve their separation and intensity should allow observation. On the other hand, the edge of the two-particle continuum appears only for very small $Q < 0.3\pi$ where magnetic intensity is very weak, as found in recent experiments [22]. We mention finally that it would be very interesting to measure the static form factors of an anisotropic chain by a method that allows one to reach the neighbourhood of $Q = \pi$, since here we are limited by the coarse-graining due to our small chains. Quantum Monte Carlo calculations, which work efficiently for static quantities, can reach this goal.

Acknowledgments

We thank S Ma *et al* for sending us a copy of [22] prior to publication. Thanks are also due to L P Regnault for discussions about neutron scattering experiments on NENP. We also thank Th Garel and J Miller for reading our manuscript.

Note added. While preparing this manuscript, we received a preprint by M Takahashi that addresses related questions.

References

- [1] Haldane F D M 1983 *Phys. Rev. Lett.* **50** 1153; 1983 *Phys. Lett.* **93A** 464
- [2] Affleck I 1989 *J. Phys.: Condens. Matter* **1** 3047
- [3] Botet R and Jullien R 1983 *Phys. Rev. B* **27** 613
Kolb M, Botet R and Jullien R 1983 *J. Phys. A: Math. Gen.* **16** L673
Botet R, Jullien R and Kolb M 1983 *Phys. Rev. B* **28** 3914; 1984 *Phys. Rev. B* **30** 215
- [4] Parkinson J B and Bonner J C 1985 *Phys. Rev. B* **32** 4703
Bonner J C 1987 *J. Appl. Phys.* **61** 3941
- [5] Moreo A 1987 *Phys. Rev. B* **35** 8562
- [6] Sakai T and Takahashi M 1990 *Phys. Rev. B* **42** 1090, 4537
- [7] Nightingale M P and Blöte H W J 1986 *Phys. Rev. B* **33** 659
- [8] Takahashi M 1989 *Phys. Rev. Lett.* **62** 2313
- [9] Deisz J, Jarrell M and Cox D L 1990 *Phys. Rev. B* **42** 4869
- [10] Golinelli O, Jolicœur Th and Lacaze R 1992 *Phys. Rev. B* **45** 9798
- [11] Affleck I, Kennedy T, Lieb E H and Tasaki H 1987 *Phys. Rev. Lett.* **59** 799; 1988 *Commun. Math. Phys.* **115** 477
- [12] Buyers W J L, Morra R M, Armstrong R L, Gerlach P and Hirakawa K 1986 *Phys. Rev. Lett.* **56** 371
Morra R M, Buyers W J L, Armstrong R L and Hirakawa K 1988 *Phys. Rev. B* **38** 543
- [13] Steiner M, Kakurai K, Kjemis J K, Petitgrand D and Pynn R 1987 *J. Appl. Phys.* **61** 3953
- [14] Tun Z, Buyers W J L, Armstrong R L, Hallman E D and Arovas D P 1988 *J. Physique Coll.* **49** Suppl 12, C8-1431
- [15] Tun Z, Buyers W J L, Armstrong R L, Hirakawa K and Briat B 1990 *Phys. Rev. B* **42** 4677
- [16] Tun Z, Buyers W J L, Harrison A and Rayne J A 1991 *Phys. Rev. B* **43** 13331
- [17] Renard J P, Verdaguer M, Regnault L P, Erkelens W A C, Rossat-Mignod J and Stirling W G 1987 *Europhys. Lett.* **3** 945
- [18] Renard J P, Regnault L P and Verdaguer M 1988 *J. Physique* C8-1425
- [19] Renard J P, Verdaguer M, Regnault L P, Erkelens W A C, Rossat-Mignod J, Ribas J, Stirling W G and Vettier C 1988 *J. Appl. Phys.* **63** 3538
- [20] Katsumata K, Hori H, Takeuchi T, Date M, Yamagishi A and Renard J P 1989 *Phys. Rev. Lett.* **63** 86
- [21] Meyer A, Gleizes A, Girerd J-J, Verdaguer M and Kahn O 1982 *Inorg. Chem.* **21** 1729
- [22] Ma S, Broholm C, Reich D H, Sternlieb B H and Erwin R W 1992 *Phys. Rev. Lett.* **69** 3571
- [23] Golinelli O, Jolicœur Th and Lacaze R 1992 *Phys. Rev. B* **46** 10854
- [24] Tsvelik A M 1990 *Phys. Rev. B* **42** 10499
- [25] Affleck I and Weston R A 1992 *Phys. Rev. B* **45** 4667
- [26] Gómez-Santos G 1989 *Phys. Rev. Lett.* **63** 790
- [27] Lieb E H and Mattis D C 1961 *J. Math. Phys.* **3** 749
Mattis D C 1985 *The Theory of Magnetism* vols I and II (Berlin: Springer)
- [28] Bender C M and Orszag S A 1987 *Advanced Numerical Methods for Scientists and Engineers* (New York: McGraw-Hill)
- [29] Gantmacher F R 1964 *Matrix Theory* (New York: Chelsea)
- [30] Regnault L P, Rossat-Mignod J and Renard J P 1992 *J. Magn. Magn. Mater.* **104** 869
- [31] Gagliano E and Balseiro C 1987 *Phys. Rev. Lett.* **59** 2999
- [32] Mikeska H J 1992 *Europhys. Lett.* **19** 39
Elstner N and Mikeska H J 1992 *Preprint*
- [33] den Nijs M and Rommelse K 1989 *Phys. Rev. B* **40** 4709
- [34] Takahashi M 1988 *Phys. Rev. B* **38** 5188
- [35] Nomura K 1989 *Phys. Rev. B* **40** 2421
Liang S 1990 *Phys. Rev. Lett.* **64** 1597
- [36] Delica T, Kopinga K, Leschke H and Mon K K 1991 *Europhys. Lett.* **15** 55